



ELSEVIER

Contents lists available at ScienceDirect

Materials Letters

journal homepage: www.elsevier.com/locate/matlet

Template-free synthesis of graphitic carbon nitride hollow spheres for photocatalytic degradation of organic pollutants

Yanjuan Cui^{a,*}, Yubin Tang^a, Xinchun Wang^b^a School of Environmental and Chemical Engineering, Jiangsu University of Science and Technology, Zhenjiang, Jiangsu 212003, PR China^b State Key Laboratory of Photocatalysis on Energy and Environment, College of Chemistry, Fuzhou University, Fuzhou 350002, PR China

ARTICLE INFO

Article history:

Received 5 July 2015

Received in revised form

20 August 2015

Accepted 22 August 2015

Available online 24 August 2015

Keywords:

Carbon nitride

Hollow sphere

Semiconductors

Microstructure

Photocatalysis

ABSTRACT

Graphitic carbon nitride ($g\text{-C}_3\text{N}_4$) hollow spheres have been prepared via one-step solvothermal method without templates. The effects of condensation temperature on the structural, optical and photocatalytic properties of the samples were investigated. The X-ray diffraction (XRD) and Fourier transformed infrared (FTIR) results show that the samples synthesized at dissimilar temperatures have graphitic and heptazine-based conjugate structure. Optical analysis results evidence that the absorption edge shifts toward longer wavelength and PL intensity quenches quickly as the treating temperature increases from 120 °C to 180 °C. The results demonstrate that higher condensation temperature improves the visible-light absorption and migration rate of photo-induced carriers of samples. The $g\text{-C}_3\text{N}_4$ sample prepared at 180 °C presents a highest photocatalytic degradation activity in the degradation of RhB under visible-light irradiation. This study demonstrates a novel strategy for one-step synthesis of hollow spheres shaped polymer semiconductor photocatalyst without templates.

© 2015 Elsevier B.V. All rights reserved.

1. Introduction

Synthesis and optimization of semiconductor photocatalysts, after nearly decades of development, have formed various sets of systematic theory and methods [1–3]. One of the challenges is to the design and development of highly active and durable heterogeneous photocatalytic materials [4,5]. Hollow nanospheres are particularly interesting because they can act as scaffolds that coassemble various functional motifs into complex nanostructures [6]. A range of inorganic and organic semiconductors with hollow structures have been synthesized via template methods employing silica, acoustic bubbles, and polymer latex. Some of these spherical and hollow semiconductors have been used in the photocatalytic reaction [7,8].

Recently, the facile synthesis and easy engineering properties render $g\text{-C}_3\text{N}_4$ a star material in the field of visible-light-driven photocatalysis. Inspired by the shape-directed functionality of semiconductors, mesoporous $g\text{-C}_3\text{N}_4$ hollow sphere has been prepared using porous silica spheres as sacrificial templates [9] and from molecular cooperative assemble method [10]. Nevertheless, this synthesis process is complicated and difficult to fabricate polymeric hollow spheres due to high temperature annealing.

For functional semiconductor synthesis, solvothermal technology could comparably simple design of material structure by using molecular engineering, solution assembly, and covalent cross-linking chemistry. Up to now, several reports have demonstrated that $g\text{-C}_3\text{N}_4$ could be prepared through direct solvothermal method under lower temperatures, and the specific morphology and microstructure of products (nanorods, nanotubes, nanowires, etc.) are easy to control [11,12].

In this work, we report template-free synthesis of $g\text{-C}_3\text{N}_4$ hollow sphere through a solvothermal method. The higher condensation temperature improves the surface area and the light absorption of samples, therefore, enhances the photocatalytic activity of samples for the degradation of RhB under visible-light irradiation.

2. Experimental section

2.1. Synthesis of $g\text{-C}_3\text{N}_4$ hollow sphere

In a typical procedure, 1,3,5-trichlorotriazine (CC, 15 mmol), dicyandiamide (DCDA, 7.5 mmol) and 60 ml acetonitrile were put into a 100-ml Teflon-lined autoclave. The mixture was stirred for 12 h, and then the autoclave was sealed and maintained at 120–180 °C for 48 h. After cooling to room temperature, the product was washed with distilled water and ethanol several times. Final products were obtained after drying at 60 °C for 12 h and denoted

* Corresponding author.

E-mail address: yjcui@just.edu.cn (Y. Cui).

as CNT, where T refers to the condensation temperature ($^{\circ}\text{C}$).

2.2. Characterization

The samples were investigated by X-ray diffraction (XRD, Bruker D8), Fourier transformed infrared spectrum (FTIR, Nicolet Magna 670), UV–vis diffuse reflectance spectrum (DRS, Varian Cary 500), X-ray photoelectron spectroscopy (XPS, Thermo ESCALAB250), scanning electron microscope (SEM, Nova NanoSEM 230) and Transmission electron microscope (TEM, Tecnai 12).

2.3. Photocatalytic activity

Photocatalytic activity tests were evaluated by the photocatalytic degradation of Rhodamine B (RhB) in an aqueous solution under visible light irradiation ($\lambda > 420 \text{ nm}$). In each experiment, 40 mg of photocatalyst was dispersed in RhB solution (80 mL, 10^{-5} mol/L). Prior to irradiation, the suspension was magnetically stirred in the dark for 30 min to reach adsorption–desorption equilibrium. The concentration of RhB was analyzed by Cary 50 UV–vis spectrophotometer at 554 nm.

3. Results and discussion

XRD patterns in Fig. 1a indicates that the distinctive graphitic-like structure exist in CN samples (indexed as JPCDS no. 87-1526). The strong peak at $\sim 27.3^{\circ}$ is a characteristic inter-layer stacking reflection of graphitic materials as the (002) peak. The other pronounced peak at $\sim 13.0^{\circ}$ can be assigned to in-plane structure

repeating motif (100) of heptazine-based g-CN [13]. With the reaction temperature increase, the intensity of these peaks becomes lower and the shape broadening. That is to say, the condensation temperature offers important effects to the physical and chemical properties of g- C_3N_4 . We can preliminary account that even under low temperature; g- C_3N_4 composed with heptazine-based structure could be produced.

FTIR spectroscopy of CN synthesized from different temperatures was shown in Fig. 1b. Contrast to the precursors CC and DCDA, the IR spectra of products are much different, indicating the polymerization reaction between them. The broad absorption band at $3100\text{--}3300 \text{ cm}^{-1}$ can be assigned to the stretching modes of secondary and primary amines and absorbed water. The band at 810 cm^{-1} and $1200\text{--}1400 \text{ cm}^{-1}$ belongs to s-triazine ring modes and characteristic aromatic heterocycles. The signals at about 2200 cm^{-1} are vested in the appearance of $\text{C}\equiv\text{N}$ or $\text{N}=\text{C}=\text{N}$, due to the incomplete polymerization of precursors [14].

In this work, the grain morphology of CN was investigated by SEM and TEM analysis, and the clear pictures of CN180 was shown in Fig. 1c and d. We can see that CN180 presents hollow sphere morphology with smooth surface, and not rule out some irregular particles. The average size distribution is about $1 \mu\text{m}$. Further research is still in progress for optimization of the morphology control of CN samples during solvothermal route.

N_2 sorption–desorption analysis revealed that the specific surface area of CN samples slightly increase from 4 to $24 \text{ m}^2 \text{ g}^{-1}$ with the synthetic temperature increase from 120°C to 180°C . For CN180, this result is much larger than that of bulk g- C_3N_4 synthesized from direct thermal polymerization at 550°C [15].

Fig. 2 gives the XPS spectra of CN180. The peaks in the C 1s

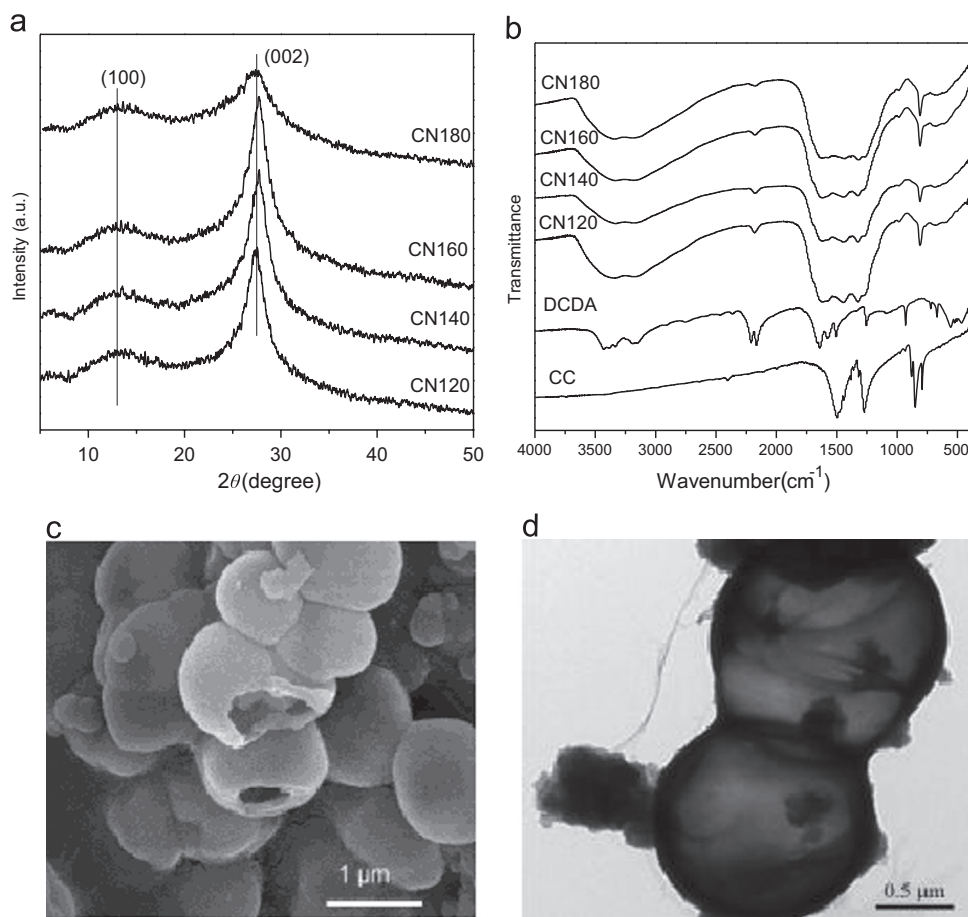


Fig. 1. XRD (a) and FTIR (b) patterns of CN samples, SEM (c) and TEM images of CN180.

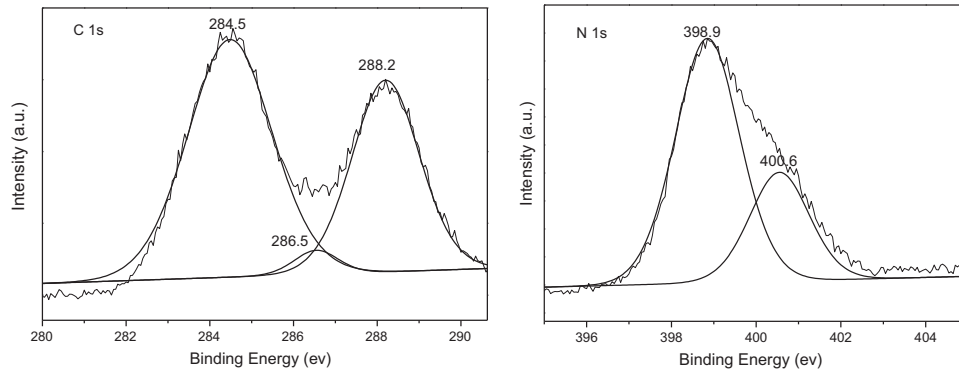


Fig. 2. High-resolution XPS spectra of C 1s, N 1s of CN180.

spectrum centered at 284.5 eV is assigned to graphitic site in the amorphous CN matrix or sp^2 C–N bond, where the peak at 285.5 eV is attributed to the sp^2 C atoms bonded to N inside the aromatic structure. The other energy contribution at 288.2 eV is assigned to sp^2 -hybridized carbon in the aromatic ring attached to the $-NH_2$ group. The N 1s spectra of sample reveal the presence of two kinds of nitrogen atom in the CN sample. The peaks at 398.9 eV is attributed to sp^2 N involved in triazine rings, while the peak at 400.6 eV is assigned to bridging N atoms N–(C)3. The absence of 401 eV reveals that the sample do not possess the N–N bonding configuration that is thought to be formed the nitrogen molecules [16]. The results clear indicate that the obtained graphitic carbon nitride hollow sphere through solvothermal method also possess typical tris-s-triazine conjugated structure.

The optical features of the as-prepared CN materials were examined by UV–vis DRS, shown in Fig. 3a. All samples have steep absorption edges in the visible light range. When the temperature increase from 120 to 180 °C, the absorption edges of products shift from 480 nm to 540 nm, corresponding to $E_g=2.36$ to 2.11 eV for CN120 to CN180. Irrefutable results can be gained that the band gap energy was much narrower than $g-C_3N_4$ obtained from traditional thermal-condensation process [17].

Fig. 3b gives the PL spectra of CN. The PL peak redshift from CN120 (centered at 505 nm) to CN180 (centered at 560 nm), which gives an indication that larger conjugated ring structures are present in solids produced. In addition, the PL intensity decrease with increasing the condensation temperature which indicates a suppressed recombination rate of the photo-induced charge carriers.

3.1. Photocatalytic performances

Fig. 4 shows the visible light photocatalytic activity of CN by degradation of organic dye RhB aqueous solution. Samples

synthesized under higher temperature performs enhanced photocatalytic degradation rate on RhB compared to $g-C_3N_4$ synthesized from bulk condensation of melamine at 550 °C. When the temperature increased to 180 °C, its photocatalytic activity enhanced greatly, and after 180 min illumination, about 100% concentration of RhB was decomposed. This may be attributed to the improved polymerization structure, extended light absorption ability and repressed charge recombination process of CN synthesized under higher temperature.

To check the photocatalytic stability of CN materials, the degradation of RhB on CN180 was repeated up to five cycles under visible light irradiation at the same conditions (Fig. 4b). After several successive operations, the sample still maintained high photocatalytic degradation activity to RhB. These results demonstrate that the presented photocatalyst with hollow sphere morphology was stable under the experimental reaction conditions.

4. Conclusions

$g-C_3N_4$ hollow sphere was successfully prepared through template-free solvothermal method. The obtained samples have typical graphitic structure and heptazine-based π -conjugated skeleton. The higher condensation temperature makes for larger surface area, wider visible-light absorption and lower recombination rate of photo-induced carriers of samples, thereby improving the photocatalytic activity for RhB degradation of the catalyst under visible light irradiation. This solvothermal route under relatively low temperature is beneficial for design and synthesis of polymer semiconductors with special morphology and microstructure.

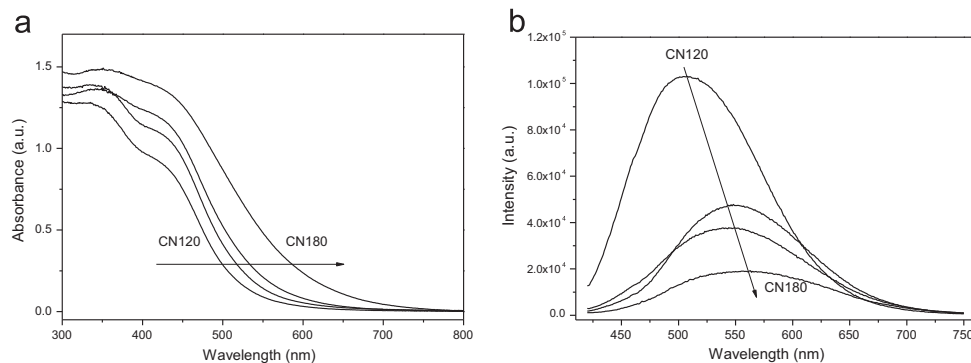


Fig. 3. (a) UV–vis DRS spectra of CN synthesized from 120 to 180 °C; (b) PL spectra of CN synthesized from 120 to 180 °C.

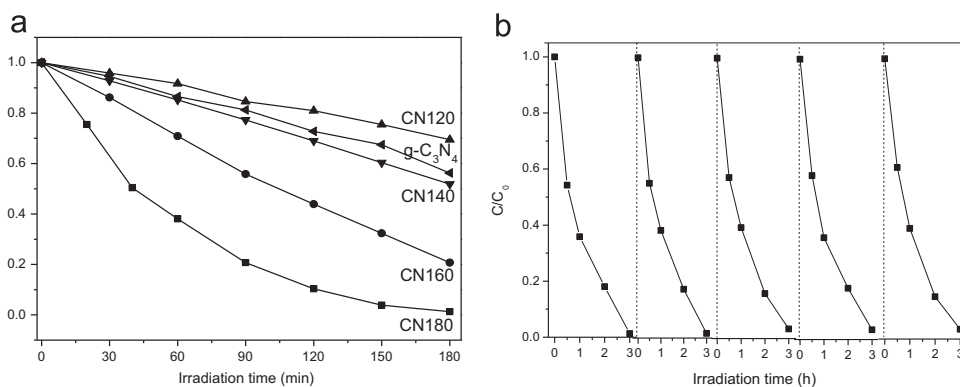


Fig. 4. Photocatalytic activity over CN (a) and the cycling runs in the presence of CN180 (b).

Acknowledgments

This work was supported by Natural Science Foundation of Jiangsu Province (Grant no. BK20140507).

References

- [1] S.C. Han, L.F. Hu, N. Gao, A.A. Al-Ghamdi, X.S. Fang, *Adv. Funct. Mater.* 24 (2014) 3725–3733.
- [2] H. Liu, X.N. Dong, L. Nan, H.X. Ma, X.J. Chen, Z.F. Zhu, *Mater. Lett.* 159 (2015) 142–145.
- [3] X.J. Xu, L.F. Hu, N. Gao, S.X. Liu, S. Wageh, A.A. Al-Ghamdi, et al., *Adv. Funct. Mater.* 25 (2015) 445–454.
- [4] J.-H. Lee, J.-I. Youn, Y.-J. Kim, H.-J. Oh, *J. Mater. Sci. Technol.* 31 (2015) 664–669.
- [5] Y. Li, W.J. Shen, *Chem. Soc. Rev.* 43 (2014) 1543–1574.
- [6] A.I. Cooper, *Adv. Mater.* 21 (2009) 1291–1295.
- [7] J. Hu, M. Chen, X.S. Fang, L.M. Wu, *Chem. Soc. Rev.* 40 (2011) 5472–5491.
- [8] Z.Y. Liu, H.W. Bai, D. Sun, *Appl. Catal. B – Environ.* 104 (2011) 234–238.
- [9] J.H. Sun, J.S. Zhang, M.W. Zhang, M. Antonietti, X.Z. Fu, X.C. Wang, *Nat. Commun.* 3 (2012) 1139–1145.
- [10] Y.S. Jun, E.Z. Lee, X.C. Wang, W.H. Hong, G.D. Stucky, A. Thomas, *Adv. Funct. Mater.* 23 (2013) 3661–3667.
- [11] Q. Gu, Y.S. Liao, L.S. Yin, J.L. Long, X.X. Wang, C. Xue, *Appl. Catal. B – Environ.* 165 (2015) 503–510.
- [12] Y.J. Cui, Z.X. Ding, X.Z. Fu, X.C. Wang, *Angew. Chem. Int. Ed.* 51 (2012) 11814–11818.
- [13] Y. Wang, X.C. Wang, M. Antonietti, *Angew. Chem. Int. Ed.* 51 (2012) 68–69.
- [14] H.Q. Li, Y.X. Liu, X. Gao, C. Fu, X.C. Wang, *ChemSusChem* 8 (2015) 1189–1196.
- [15] Y.J. Cui, J.S. Zhang, G.G. Zhang, J.H. Huang, P. Liu, M. Antonietti, et al., *J. Mater. Chem.* 21 (2011) 13032–13039.
- [16] A. Vinu, *Adv. Funct. Mater.* 18 (2008) 816–827.
- [17] Y. Zheng, J. Liu, J. Liang, M. Jaroniec, S.Z. Qiao, *Energy Environ. Sci.* 5 (2012) 6717–6731.